RESEARCH PAPER

Effect of deviator stress on the initiation of suffusion

Yulong Luo[1] · Bin Luo[1] · Ming Xiao[2]

Abstract

Stress state has significant influence on the initiation of suffusion, whereas the effect of deviator stress has not been investigated thoroughly. This paper presented a series of hydro-mechanical coupling suffusion tests on four internally unstable cohesionless soils to investigate the effect of deviator stress on the initiation of suffusion. A dimensionless parameter, shear stress ratio, which is the ratio of deviator stress to mean effective stress, was introduced to denote the variation of deviator stress under the same confining pressure. The results indicate that the deviator stress or shear stress ratio has significant influence on the initiation of suffusion. The relationship between shear stress ratio and critical hydraulic gradient initiating suffusion is piecewise linear, and there is a critical shear stress ratio for different internally unstable soils. The critical hydraulic gradient first linearly increases with the increase in shear stress ratio, and it reaches the maximum value at the critical shear stress ratio, then it decreases suddenly and significantly, finally it increases linearly again with the increase in shear stress ratio. The critical shear stress ratio is not the division between volumetric contraction and dilation, but it can be determined by a consolidated drained triaxial compression test. Based on the characteristic of the relationship between shear stress ratio and critical hydraulic gradient, an empirical method determining the critical hydraulic gradients under complex stress states was developed.

Keywords Critical hydraulic gradient · Deviator stress · Hydro-mechanical · Initiation of suffusion · Internally unstable

1 Introduction

Suffusion, a type of subsurface or internal erosion, refers to the migration of fine particles in a coarser soil matrix. Some embankment dam distresses or failures are associated with suffusion [5, 7, 28]. For suffusion to occur, the following two criteria have to be satisfied: (a) a geometrical criterion: gap-graded cohesionless soil and broadly graded cohesionless soil with a flat "tail" of fine particle gradation are typical internally unstable soils and prone to suffusion [31, 32, 35]; (b) a hydro-mechanical criterion: the initiation of suffusion is governed by the influence of the hydraulic gradient and effective stress within the soil [6, 7, 20–22, 25]. This paper focused on the hydro-mechanical criterion, and the objective was to investigate the influence of deviator stress on the initiation of suffusion. A dimensionless parameter, shear stress ratio (η), was adopted to denote the variation of deviator stress under the same confining pressure. The shear stress ratio was introduced by Chang and Zhang [7], and it is the ratio of deviator stress q ($q = \sigma_1 - \sigma_3$, where σ_1 and σ_3 are the major and minor principal stress, respectively) to mean effective stress p' ($p' = (\sigma_1 + 2\sigma_3)/3$).

The critical hydraulic gradient, at which suffusion initiates, has been studied comprehensively. Initially, the effect of stress state on the initiation of suffusion was not considered. Skempton and Brogan [30] found that the critical hydraulic gradient in internally unstable sandy gravel was far lower than that given by Terzaghi, and postulated that a major portion of effective stress was carried by coarse particles, leaving fine particles under

✉ Yulong Luo
  lyl8766@hhu.edu.cn

  Bin Luo
  seepagehhu@126.com

  Ming Xiao
  mxiao@engr.psu.edu

[1] College of Water Conservancy and Hydropower Engineering, Hohai University, Nanjing 210098, China

[2] Department of Civil and Environmental Engineering, The Pennsylvania State University, University Park, PA 16802, USA

relatively small pressures. Based on this postulation, a new concept of stress reduction factor was proposed to characterize the effective stress transferred by fine particles. Recently, the initiation of suffusion under uniaxial load was also studied. Moffat and Fannin [25] proposed a novel concept of a hydro-mechanical path in stress-gradient space associated with suffusion and found that the critical hydraulic gradient initiating suffusion increased with the increase in mean vertical effective stress. Based on the new concept, a formula for the critical hydraulic gradient denoted by a normalized mean vertical effective stress was developed by Li and Fannin [20]. Moffat and Herrera [27] proposed a theoretical model to determine the critical hydraulic gradient, which was related to vertical effective stress, porosity, friction angle between coarse and fine particles, and the stress reduction factor proposed by Skempton and Brogan [30]. Luo et al. [22] investigated suffusion at the bottom of a cutoff wall in an internally unstable sandy gravel alluvium based on flume-scale experiments. The results suggested that the critical hydraulic gradient linearly increased with the increase in overburden pressure, and a linear empirical formula for the critical hydraulic gradient was derived. However, internally unstable soils in the field are always under complex stress states [7, 21], and influences of confining pressure and deviator stress on the initiation of suffusion should be considered simultaneously. The research performed by Chang and Zhang [7] highlighted the effect of deviator stress or shear stress ratio on the critical hydraulic gradient. Their results as shown in Fig. 1 revealed the following interesting observations: (a) for the gap-graded soil in their study, the critical hydraulic gradient first linearly increased with the shear stress ratio; after reaching a critical shear stress ratio (η_{cr}), it started to decrease with the shear stress ratio until the stress conditions approached failure; (b) the critical shear stress ratio was approximately 1.2, and the

critical hydraulic gradient reached the maximum value at the critical shear stress ratio.

Based on Fig. 1 as observed by Chang and Zhang [7], three important questions deserve further investigation. (a) Is the effect of shear stress ratio on the critical hydraulic gradient similar for different internally unstable soils? (b) Is the critical shear stress ratio equal to 1.2 for different internally unstable soils? Is the critical shear stress ratio the division between volumetric contraction and dilation? (c) How to determine the critical hydraulic gradient for any internally unstable soil under complex stress states in the field? The answers to these questions bear significance on engineering applications, such as design and evaluation of high earthen and rockfill dams constructed on internally unstable soils [5, 22].

To answer the above questions, four internally unstable soils were tested. Thirty-six suffusion tests under different shear stress ratios and four triaxial compression tests on the four original soils without suffusion were performed to investigate the effect of shear stress ratio on critical hydraulic gradient. An empirical method determining the critical hydraulic gradients under different shear stress ratios was developed based on the experimental results.

2 Methodology

2.1 Characteristics of the testing soils

In this study, three gap-graded cohesionless soils (soils A, B, C) with different fine particle contents and one broadly graded cohesionless soil (soil D) were tested. Figure 2 depicts the grain size distributions of the four soils. For soils A, B, C, and D, the coefficients of uniformity are 22.2, 27.1, 30.0, and 25.8, respectively, and the coefficients of curvature are 8.0, 9.5, 9.3, and 6.7, respectively. According to several geometric criteria [8, 16, 19, 33], the four soils are internally unstable soils. The assessment of internal stability using these criteria is shown in Table 1. Based on
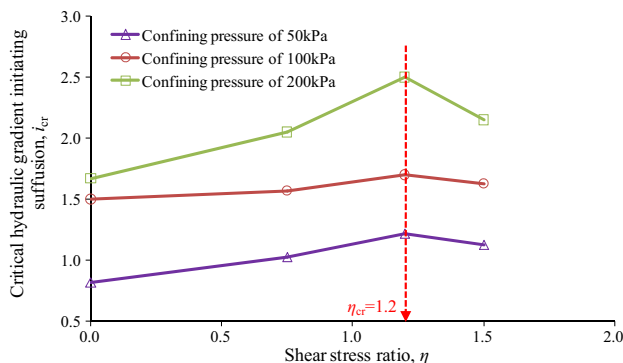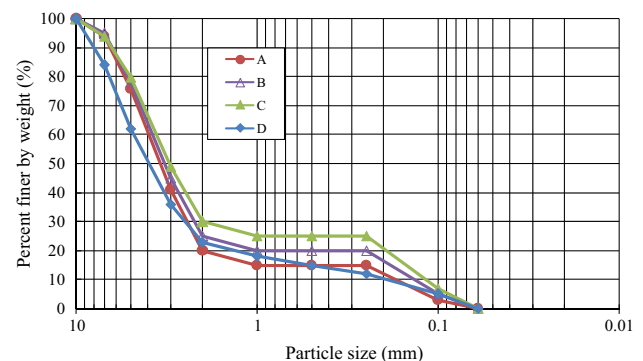

Fig. 1 Relationship between shear stress ratio and the critical hydraulic gradient initiating suffusion (it was redrawn based on Fig. 13(b) in Chang and Zhang [7])

Fig. 2 Grain size distributions of the testing soils

Table 1 Evaluation of internal instability of the testing soils

Criteria	Material description	The soil is internally stable if	Internally unstable			
			A	B	C	D
Kenney and Lau [16]	Granular soils	$(H/F)_{min} > 1$	Y	Y	Y	Y
		For broadly graded soil, $0 < F < 20\%$; For narrowly graded soil, $0 < F < 30\%$				
Wan and Fell [33]	Broadly graded and gap-graded soils	$P = e^Z/[1 + e^Z]$	Y	Y	Y	Y
		$Z = 3.875\log(h'') - 3.591\ h' + 2.436$ for sand-gravel mixtures				
Li and Fannin [19]	Granular soils	For $F < 15\%$, $(H/F)_{min} \geq 1.0$	Y	Y	Y	Y
		For $F > 15\%$, $H \geq 15\%$				
Chang and Zhang [8]	Broadly graded soils	$P' < 5$, $(H/F)_{min} > 1.0$	Y	Y	Y	Y
		$5 \leq P' \leq 20$, $(H/F)_{min} > -(1/15)P' + 4/3$				
		$P' > 20$, stable				

F = mass fraction at any grain size d; H = mass fraction between grain size d and $4d$; P = probability of internal instability; $h' = d_{90}/d_{60}$; $h'' = d_{90}/d_{15}$; d_{90}, d_{60}, and d_{15} = diameters of 90%, 60%, and 15% mass passing, respectively; P' = fine particle content (< 0.063 mm); Y = internally unstable

the method proposed by Wan and Fell [32], for broadly graded soils, the division between coarse and fine particles could be found at the point on the grain size distribution with $(H/F)_{min}$, which was defined by Kenney and Lau [16]. For gap-graded soils, $(H/F)_{min}$ could be found at the gap location. Consequently, fine particles in the gap-graded soils A, B, and C in this study refer to the particles finer than 0.25 mm, whereas in the broadly graded soil D, fine particles are the particles finer than 0.5 mm, and the corresponding fine particle contents for soils A, B, C, and D are 15%, 20%, 25%, and 15%, respectively.

2.2 Stress-controlled suffusion apparatus

The testing apparatus is a stress-controlled suffusion apparatus, as depicted in Fig. 3. It is similar to the apparatus designed by Bendahmane et al. [6] and Chang and Zhang [7]. Such apparatus can investigate the evolution of suffusion under different stress states and hydraulic gradients. Meanwhile, it can perform consolidated drained triaxial compression test. The apparatus mainly consists of a confining pressure system, an axial loading system, a seepage pressure system, a funnel-shaped drainage system, and a data acquisition system. The confining pressure and axial loading systems simulate the stress state of specimen. The largest confining pressure and axial load are 2.0 MPa and 30 kN, respectively. The seepage pressure system provides downward seepage for the migration of fine particles. The total head difference across specimen is controlled by a water tank with adjustable height. The funnel-shaped draining system with a covering screen is specially designed to allow fine particles to be washed out of the

specimen freely; meanwhile, it does not affect the standard operation of triaxial compression test. Pore-opening size of the covering screen may have significant influence on the migration of fine particles. A suitable pore-opening size, which can allow the eroded fine particles to be washed out of the funnel-shaped drainage system freely, is critical for suffusion test. The ratio of the pore-opening size to the largest fine particle size, R_p, ranges from 6.7 to 28.5 in previous studies [7, 15, 26]. In this study, the pore-opening size is 4 mm, and the largest fine particle size is 0.25 mm for soils A, B, and C, and it is 0.5 mm for soil D. Therefore, $R_p = 16$ (for soils A, B, and C) or $R_p = 8$ (for soil D). It can be concluded that the adopted pore-opening size is suitable for suffusion tests. The data acquisition system can monitor the mass of eroded fine particles, settlement, volume change, and total head difference of the specimen. Hydraulic gradient is determined by the ratio of the total head difference to the length of the specimen. Flow velocity is measured manually. The detailed information on this apparatus can be found in Luo et al. [23].

2.3 Suffusion test procedure

Table 2 shows the summary of suffusion tests. Thirty-six tests were carried out, and all the tests were conducted in the following five steps. (1) Specimen preparation: Each specimen was compacted in five layers, and the moist-tamping method was adopted to minimize particle segregation [17]. The dimensions of the specimen in this study are similar to those in Chang and Zhang [7], and they are 101 mm in diameter and 100 mm in height. It should be noted that the reliability of test significantly depends on the
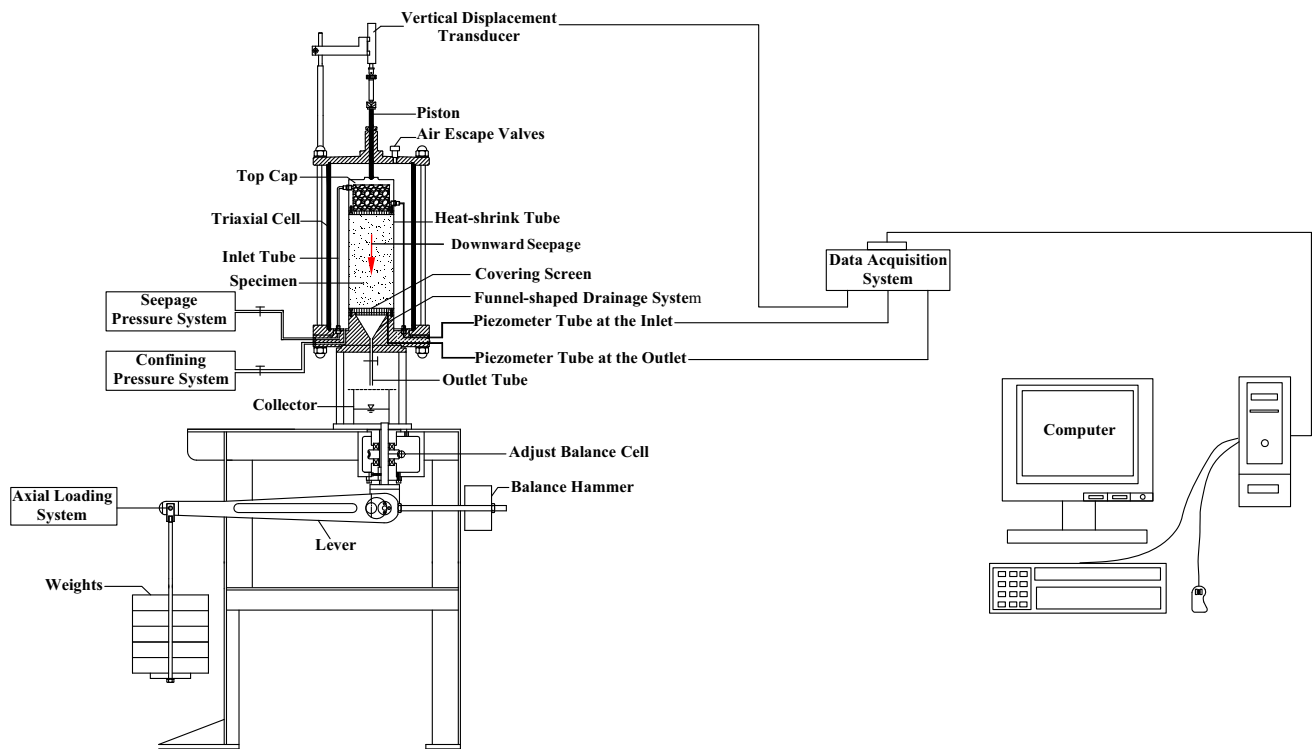
Fig. 3 Stress-controlled suffusion apparatus

ratio of the specimen diameter (D_s) to the largest particle size (d_{max}) of testing soil. According to ASTM D5084-10 [2], ASTM D7181-11 [4], and ASTM D3999/D3999 M-11 [3], the specimen diameter should be at least six times the largest particle size of the specimen. In addition, some researchers have suggested that a ratio of 5 for the specimen diameter and the largest particle size was sufficient to avoid scale effect [10, 12, 24]; some researchers also have suggested that a ratio of 6 to 8 was considered necessary for meaningful results [9, 11]. In this study, the value of D_s/d_{max} is equal to 10.1, so it can be concluded that the value of D_s/d_{max} in this study is sufficient to avoid scale effect of tests. The desired dry densities of soils A, B, C, and D are 1.85 g/cm^3, 1.87 g/cm^3, 1.88 g/cm^3, and 1.88 g/cm^3, respectively, and the relative density is approximately 0.27. The designated initial porosities are 0.30, 0.29, 0.28, and 0.29, respectively. (2) Saturation: A differential water-head method was adopted to saturate specimen. To ensure a high degree of saturation, carbon dioxide was first injected into the specimen to flush trapped air, and then de-aired water was gradually introduced until inflow rate was equal to outflow rate. Saturation time in every test was approximately three hours. (3) Consolidation at a controlled stress state: Consolidation was gradually conducted by increasing confining pressure to the designated value of 0.4 MPa, and then deviator stress gradually increased to the desired value after the specimen was isotropically consolidated. (4)

Suffusion test: After the required stress state had been applied, suffusion test started, and a step-increase hydraulic gradient was introduced into the specimen. Based on the previous studies, such as Skempton and Brogan [30], Wan and Fell [32], and Ke and Takahashi [14], the critical hydraulic gradient initiating suffusion is indeed low. In Ke and Takahashi [14], for the internally unstable soils with initial fine particle contents of 14.3%, 16.7%, 20%, and 25%, the corresponding critical hydraulic gradient are 0.21, 0.23, 0.24, and 0.25, respectively. The low value of the critical hydraulic gradient may be attributed to the heterogeneity of stress transfer in internally unstable soils. Fine particles in internally unstable soils only transfer a little or no effective stress, while coarse particles mainly transfer effective stress [16, 22, 30]. In order to capture the low critical hydraulic gradient initiating suffusion (i_{cr}), the suffusion tests here started with a slow gradual increase in the hydraulic gradient until suffusion initiated. For example, hydraulic gradient increased by 0.05 per 30 min in the first few steps. When hydraulic gradient exceeded i_{cr}, suffusion had initiated, and the rate of gradient increase could increase gradually to accelerate the process of the suffusion tests (i.e., 0.1 per 30 min for $i_{cr} < i \leq 1.0$, 0.2 per 30 min for $1.0 < i < 2.0$, and 0.5 per 30 min for $i \geq 2.0$). In every step, migration of fine particles and turbidity of effluent were observed closely. Simultaneously, flow velocity and the total heads at the inlet and outlet were recorded in

Table 2 Summary of the suffusion tests under different deviator stresses

Test no.	Dry density (g/cm^3)	Relative density	Initial porosity	Applied stress state			
				Confining pressure, σ_3 (MPa)	Deviator stress, q (MPa)	Mean effective stress, p' (MPa)	Shear stress ratio, $\eta = q/p'$
A-1	1.85	0.27	0.30	0.4	0	0.40	0
A-2			0.30		0.1	0.43	0.23
A-3			0.30		0.2	0.47	0.43
A-4			0.30		0.4	0.53	0.75
A-5			0.30		0.6	0.60	1.0
A-6			0.29		0.7	0.63	1.11
A-7			0.30		0.8	0.67	1.20
A-8			0.30		1.0	0.73	1.36
A-9			0.30		1.2	0.80	1.50
B-1	1.87	0.27	0.29		0	0.40	0
B-2			0.29		0.1	0.43	0.23
B-3			0.30		0.2	0.47	0.43
B-4			0.29		0.4	0.53	0.75
B-5			0.29		0.6	0.60	1.0
B-6			0.29		0.7	0.63	1.11
B-7			0.30		0.8	0.67	1.20
B-8			0.29		1.0	0.73	1.36
B-9			0.29		1.2	0.80	1.50
C-1	1.88	0.27	0.28	0.4	0	0.40	0
C-2			0.28		0.1	0.43	0.23
C-3			0.28		0.2	0.47	0.43
C-4			0.28		0.4	0.53	0.75
C-5			0.28		0.6	0.60	1.0
C-6			0.29		0.7	0.63	1.11
C-7			0.28		0.8	0.67	1.20
C-8			0.28		1.0	0.73	1.36
C-9			0.28		1.2	0.80	1.50
D-1	1.88	0.27	0.29	0.4	0	0.40	0
D-2			0.28		0.1	0.43	0.23
D-3			0.29		0.2	0.47	0.43
D-4			0.29		0.4	0.53	0.75
D-5			0.29		0.6	0.60	1.0
D-6			0.29		0.7	0.63	1.11
D-7			0.29		0.8	0.67	1.20
D-8			0.29		1.0	0.73	1.36
D-9			0.28		1.2	0.80	1.50

10-min interval. If flow velocity and the total heads no longer changed and no further soil loss was observed, the next step of hydraulic gradient was applied. (5) Sieve analyses: After each test, grain size distributions of the specimen and the eroded particles in every step were determined by sieve analysis according to ASTM D6913-04 [1]. The eroded particles in each step were separately collected and dried after the test, and then the eroded mass was recorded as instantaneous eroded mass.

2.4 Determination of the critical hydraulic gradient initiating suffusion

Based on Chang and Zhang [7], the entire suffusion process can be divided into four phases: stable, initiation,

development, and failure. At present, the critical hydraulic gradient initiating suffusion is not well defined, and the definitions are different in the different literature. Skempton and Brogan [30] suggested the critical hydraulic gradient was the one at which violent piping of fine particles and a rapid increase in inflow occurred. Wan and Fell [32] defined that the critical hydraulic gradient corresponded to the hydraulic gradient at which the first sign of erosion of fine particles was observed. Recent studies included more specific definitions. Ke and Takahashi [14] postulated that suffusion initiated when the relationship between hydraulic gradient and flow velocity begun to inflect; meanwhile, ''dance-like'' movements of fine particles were first observed. Similarly, Chang and Zhang [7] defined that the initiation gradient was the minimum hydraulic gradient in the initiation phase where there was some loss of fine particles and a slight change in permeability.

Comparing to the definitions in the different literature, it can be found that some definitions rely on the observation of eroded particles and partly depend on the subjectivity of observers. The recently proposed definitions are more precise since they involve more details about the initiation of suffusion [7, 14]. So the definitions in Ke and Takahashi [14] and Chang and Zhang [7] were adopted in this study to determine the critical hydraulic gradient initiating suffusion.

2.5 Test procedure of consolidated drained triaxial compression

Suffusion is a localized phenomenon, and capturing the critical hydraulic gradient initiating suffusion in test is a great challenge. Actually, the specimen in this study, which is only 101 mm in diameter and 100 mm in height, is small. When suffusion initiated, the average hydraulic gradient of the specimen, which is determined by the ratio of the total head difference across the specimen to the height of the specimen, could be representative of the localized hydraulic gradient initiating suffusion. So the global porosity of the specimen in this study is helpful for explaining the variation of the critical hydraulic gradient under different shear stress ratios. In addition, Chang and Zhang [7] also deemed that the variation of the critical hydraulic gradient initiating suffusion was mainly caused by the variation of soil porosity under different shear stress ratios.

In order to investigate the variation of soil porosity under different shear stress ratios, four consolidated drained triaxial compression tests on the original soils A, B, C, and D without suffusion were also performed by the stress-controlled suffusion apparatus in this study according to ASTM D7181-11 [4]. The specimens for the compression tests had the same dimensions, initial porosity, dry

density, and confining pressure as the suffusion specimens. Conventionally, the aspect ratio of the specimen should be 2:1 for conventional triaxial compression test. However, the use of the specimen aspect ratio of 1:1 in this study was based on two considerations. First, the aspect ratio is recommended as 1:1 for seepage tests in a triaxial cell, in standard BS1377 of the British Standards Institution [7]. Second, the main purpose of the triaxial compression test in this study was to investigate the variations of soil porosity under different deviator stresses, not the stress-strain relationship.

The specimen was first consolidated to the designated confining pressure of 0.4 MPa, and then deviator stress was gradually increased until shear failure occurred. In this study, a new parameter termed as rate of volumetric change, $\Delta V/\Delta q$, was introduced to characterize the variations of soil porosity under different shear stress ratios. The value of $\Delta V/\Delta q$ is the ratio of volumetric change to the increment of deviator stress. A negative sign of $\Delta V/\Delta q$ denotes volumetric contraction, and a plus sign of $\Delta V/\Delta q$ denotes volumetric dilation.

3 Results and discussion

3.1 Determination of the initiation of suffusion in test D-6

It is noted that only the results of test D-6 were described comprehensively in this section. The test condition of D-6 is listed in Table 2. Similar results and evolution trends in terms of hydraulic gradient and flow velocity also appeared in the other thirty-five suffusion tests. Figure 4 depicts the relationships between hydraulic gradient (i) and flow velocity (v), and instantaneous eroded mass (m_e) in test D-6. It can be seen that the relationship between i and v in the evolution of suffusion was piecewise linear, and the whole process of the test could be divided into six phases
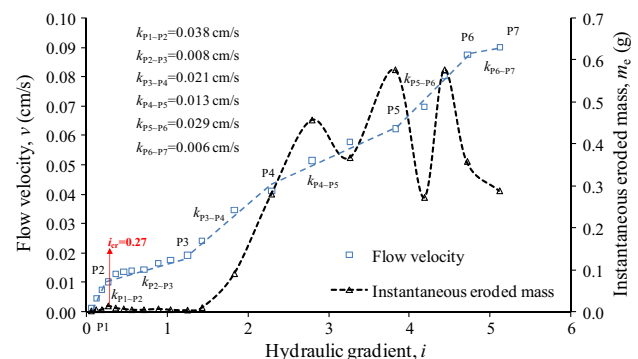

Fig. 4 Relationships between hydraulic gradient and flow velocity, and instantaneous eroded mass (test D-6)

(i.e., P1–P2, P2–P3, P3–P4, P4–P5, P5–P6, and P6–P7). In each phase, v increased linearly with the increase of i, and the specimen permeability, which was the slope of i–v curve, was approximately constant. The permeability of soil in the six phases was approximately 0.038 cm/s, 0.008 cm/s, 0.021 cm/s, 0.013 cm/s, 0.029 cm/s, and 0.006 cm/s, respectively. The first change in permeability initiated at P2 where hydraulic gradient was 0.27. Meanwhile, noticeable migration of fine particles was also observed in the transparent outlet tube, and the instantaneous eroded mass at $i = 0.27$ significantly increased to 0.01 g. According to the definitions of i_{cr} proposed by Ke and Takahashi [14] and Chang and Zhang [7], it could be judged that suffusion initiated at $i_{cr} = 0.27$.

In addition, it can be seen from Fig. 4 that the relationship between hydraulic gradient (i) and instantaneous eroded mass (m_e) could explain the variation of permeability in the evolution of suffusion. The variation of permeability was attributed to fine particle migration and subsequent clogging within the specimen. At the initiation of suffusion, some fine particles started to migrate, and consequently they clogged pores within the specimen, this caused a decrease in permeability. The permeability in the first phase (k_{P1-P2}) was 0.038 cm/s, whereas k_{P2-P3} was 0.008 cm/s. In the third phase (P3–P4), m_e started to increase significantly to 0.28 g at $i = 2.29$, and k_{P3-P4} increased to 0.021 cm/s, it indicated that clogged pores were unclogged. In the fourth phase (P4–P5), m_e started to fluctuate, the instantaneous eroded masses were 0.46 g at $i = 2.79$, 0.37 g at $i = 3.26$, and 0.58 g at $i = 3.82$; k_{P4-P5} decreased to 0.013 cm/s. In the fifth phase (P5–P6), k_{P5-P6} increased to 0.029 cm/s. In the sixth phase (P6–P7), pores within the specimen were clogged again by the migration of fine particles, which induced a significant decrease of permeability to 0.006 cm/s. It can be inferred that the evolution of suffusion was a complicated process, and it involved fine particles migration, pores clogging, pores unclogging, and fine particles remigration. The similar phenomena were also observed by Sibille et al. [29], Le et al. [18], Hu et al. [13], and Yang et al. [34].

3.2 Effect of shear stress ratio on the critical hydraulic gradient

Figure 5 shows the relationships between shear stress ratio (η) and the critical hydraulic gradient initiating suffusion (i_{cr}) of the four internally unstable soils. It can be seen that the deviator stress or shear stress ratio had significant influence on the critical hydraulic gradient. The relationship between η and i_{cr} was piecewise linear, and there was a critical shear stress ratio (η_{cr}) for each soil in this study. The value of i_{cr} first linearly increased with the increase of η when η was less than η_{cr}, and it reached the maximum
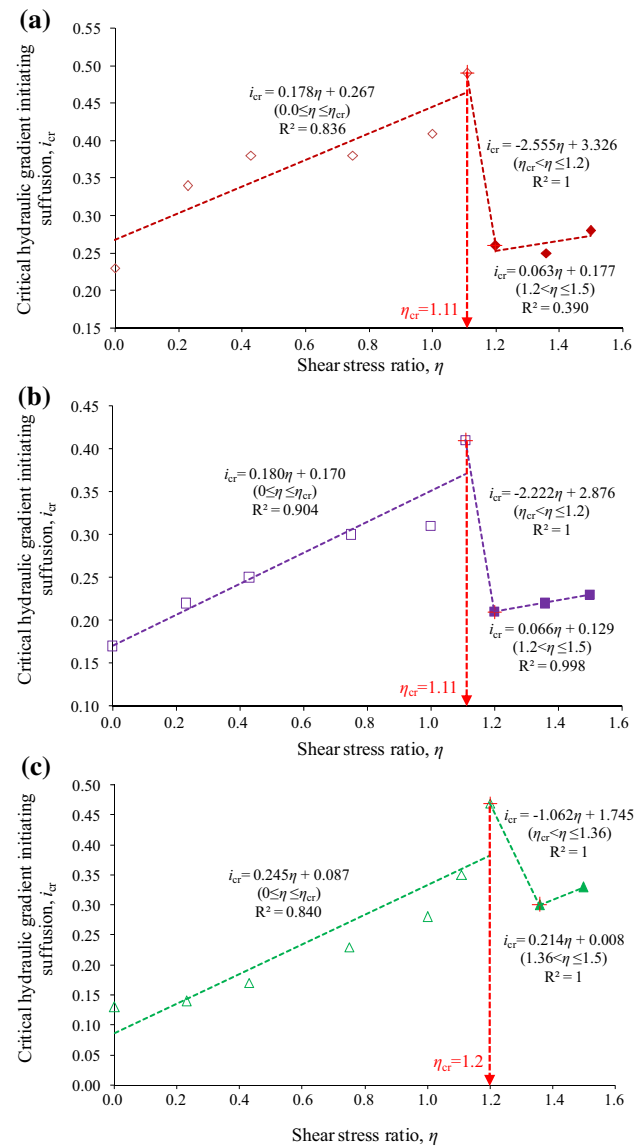

Fig. 5 Relationships between shear stress ratio and critical hydraulic gradient initiating suffusion: **a** soil A; **b** soil B; **c** soil C; **d** soil D

value at $\eta = \eta_{cr}$, then it decreased suddenly and significantly just over η_{cr}, finally it increased linearly again with the increase of η when η was larger than η_{cr}. The critical shear stress ratios of the four soils A, B, C, and D are rather similar, and they are 1.11, 1.11, 1.2, and 1.0, respectively.

Compared with Fig. 1 observed by Chang and Zhang [7], the results depicted in Fig. 5 indicated two common features and one significant distinction. The two common features are: (a) there was a critical shear stress ratio for each internally unstable soil (three gap-graded soils and one broadly graded soil in this study, while one gap-graded soil in Chang and Zhang [7]); (b) the value of i_{cr} linearly increased with the increase of η when η was less than η_{cr}, and i_{cr} reached the maximum value at $\eta = \eta_{cr}$. The significant distinction was the variation of i_{cr} when η was
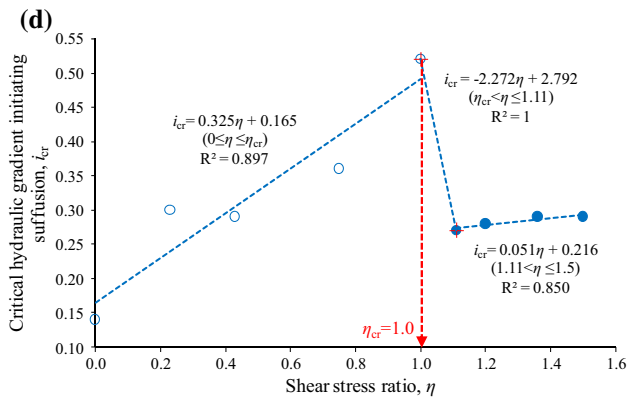
Fig. 5 continued

larger than η_{cr}. The results observed by Chang and Zhang [7] suggested that η_{cr} corresponded to the stress condition approaching failure, and i_{cr} started to decrease linearly when η was larger than η_{cr}, whereas the results in this study indicated that i_{cr} first decreased suddenly and significantly with a slight increase of η, and then it linearly increased with the increase in η.

In addition, it was found that fine particle content also had influence on the critical hydraulic gradient. For soils A, B, and C with different fine particle contents (15%, 20%, and 25%, respectively), i_{cr} decreased with the increase in fine particle content under the same shear stress ratio when η was less than 1.11. For example, at $\eta = 0.43$, the critical hydraulic gradients of soils A, B, and C were 0.38, 0.25, and 0.17, respectively. The similar effect of fine particle content on i_{cr} was also observed by Ke and Takahashi [14].

3.3 Explanation on the variation of critical hydraulic gradient

Figure 6 shows the relationships between shear stress ratio (η) and volumetric strain (ε_v), and rate of volumetric change ($\Delta V/\Delta q$). On one hand, Fig. 6 can explain the variation of i_{cr} with the increase in shear stress ratio, as depicted in Fig. 5. On the other hand, it can be used to investigate the significant distinction between this study and Chang and Zhang [7]. It can be seen from Fig. 6 that ε_v first decreased with the increase of η, and then it reached the minimum value at $\eta = \eta_d$, which was the division between volumetric contraction and dilation, finally ε_v started to increase with the increase of η. For soils A, B, C, and D, the values of η_d are 1.71, 1.81, 1.72, and 2.0, respectively. Compared with Fig. 5, it was found that the maximum critical hydraulic gradients depicted in Fig. 5 did not occur at $\eta = \eta_d$.
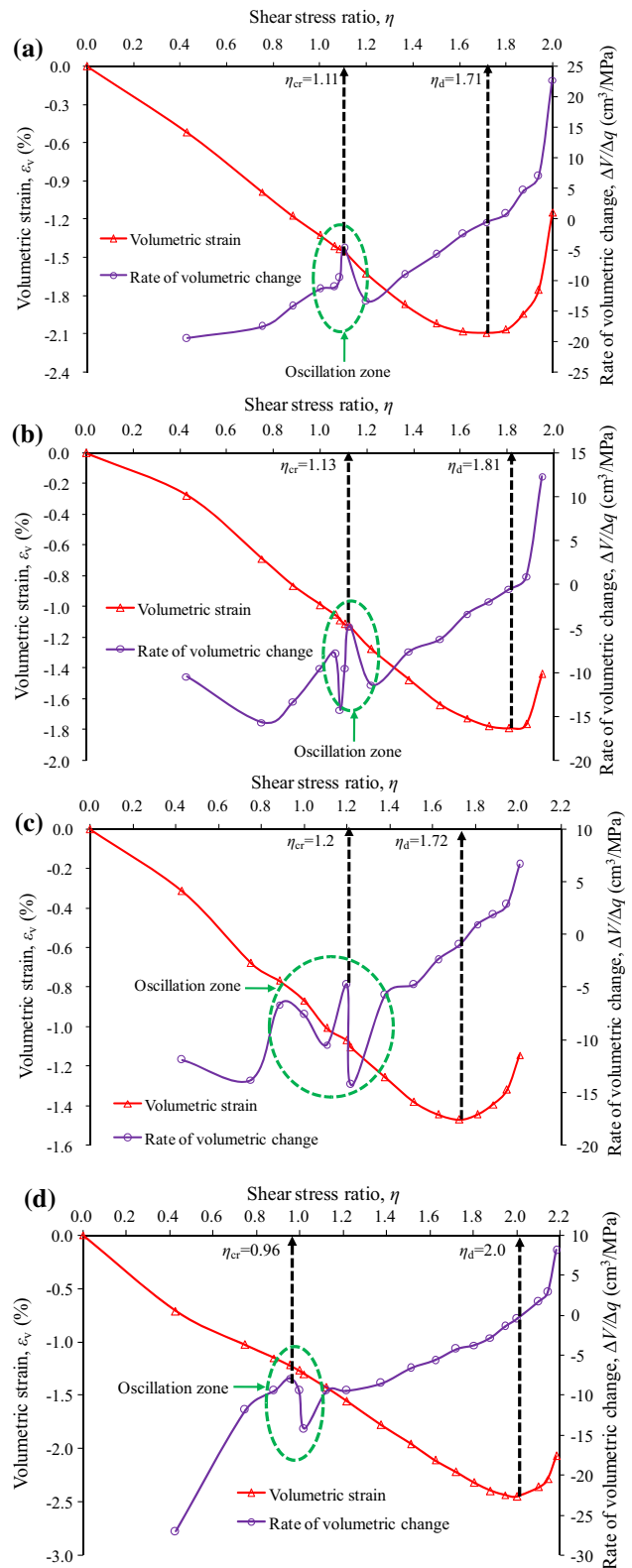

Fig. 6 Relationships between shear stress ratio and volumetric strain, and rate of volumetric change: **a** soil A; **b** soil B; **c** soil C; **d** soil D

The variations of $\Delta V/\Delta q$ were significantly different from those of ε_v. For each soil, there was an interesting oscillation zone, as depicted in Fig. 6. In the oscillation zone, there was a maximum value of $\Delta V/\Delta q$ at $\eta = \eta_{cr}$. For the four soils A, B, C, and D, the critical shear stress ratios determined by the consolidated drained triaxial compression tests are 1.11, 1.13, 1.20, and 0.96, respectively. Compared with Fig. 5, it was found that the critical shear stress ratios determined by the suffusion tests (as shown in Fig. 5) were significantly consistent with those determined by the consolidated drained triaxial compression tests (as shown in Fig. 6). Therefore, it can be concluded that the critical shear stress ratio is not the division between volumetric contraction and dilation, and it does not correspond to the stress condition approaching failure, but it is the point where $\Delta V/\Delta q$ reaches the maximum value in the oscillation zone, and it is still in volumetric contraction state, as depicted in Fig. 6.

Based on Figs. 5 and 6, the variations of i_{cr} under different shear stress ratios may be attributed to the variation of soil porosity. When η was less than η_{cr}, the specimen gradually contracted with the increase of η, and soil porosity decreased gradually, and this seriously hindered the migration of fine particles and induced the increment of i_{cr} with the increase of η. At $\eta = \eta_{cr}$, the specimen was still in contraction state, and $\Delta V/\Delta q$ reached the maximum value, and the corresponding soil porosity reached the minimum value in the oscillation zone, and consequently, i_{cr} was up to the maximum value at $\eta = \eta_{cr}$. In the oscillation zone, $\Delta V/\Delta q$ started to decrease significantly and suddenly with a slight increase of η when η was larger than η_{cr}, and the corresponding soil porosity significantly and suddenly increased from the minimum value, so i_{cr} decreased significantly. The oscillation of $\Delta V/\Delta q$ around η_{cr} in Fig. 6 intuitively depicted the variation of i_{cr} around η_{cr} in Fig. 5. When η was larger than η_{cr} and less than η_d, the specimen was not in the oscillation zone, but it was still in contraction state. The value of $\Delta V/\Delta q$ increased with the increase of η, and soil porosity started to decrease gradually with the increase of η; consequently, i_{cr} started to increase again with the increase of η until the stress condition caused dilation at $\eta = \eta_d$. When η was larger than η_d, the specimen started to be in dilation state, and $\Delta V/\Delta q$ increased with the increase of η, and soil porosity started to increase gradually with the increase of η; consequently, i_{cr} started to decrease with the increase of η. In the field, once the stress condition starts to cause volumetric dilation, it means that the soil has approached failure, so the variation of i_{cr} is not discussed when η is larger than η_d.

3.4 An empirical method determining the critical hydraulic gradients under complex stress states

Compared with the results in this study and Chang and Zhang [7], it was found that for different internally unstable soils with different grain size distributions and fine particle contents, the effect of shear stress ratio on the critical hydraulic gradient initiating suffusion was similar, as depicted in Fig. 5. According to this characteristic, an empirical method determining the stress-dependent critical hydraulic gradients under complex stress states was developed. The detailed procedures are as follows:

1. Based on the stress states (i.e., confining pressure and deviator stress) of the testing soil, one consolidated drained triaxial compression test under the same confining pressure was carried out to determine η_{cr}. According to Sect. 3.3, η_{cr} is not the division between volumetric contraction and dilation, but it is the point where $\Delta V/\Delta q$ reaches the maximum value in the oscillation zone.

2. Four suffusion tests under the same confining pressure and different shear stress ratios were performed to determine i_{cr}. For example, test A1 with $\eta = \eta_1$ and $i_{cr} = i_{cr1}$, test A2 with $\eta = \eta_2 = \eta_{cr}$ and $i_{cr} = i_{cr2}$, test A3 with $\eta = \eta_3$ and $i_{cr} = i_{cr3}$, and test A4 with $\eta = \eta_4$ and $i_{cr} = i_{cr4}$ ($\eta_4 \le \eta_d$, where η_d is the division between volumetric contraction and dilation), as depicted in Fig. 7.

3. The stress-dependent critical hydraulic gradients under different shear stress ratios were established by piecewise linear interpolations between η_1 and η_2, η_2 and η_3, and η_3, and η_4, as shown in Fig. 7. The parameters a_1–a_6 were determined by linear interpolations of the four suffusion tests results.
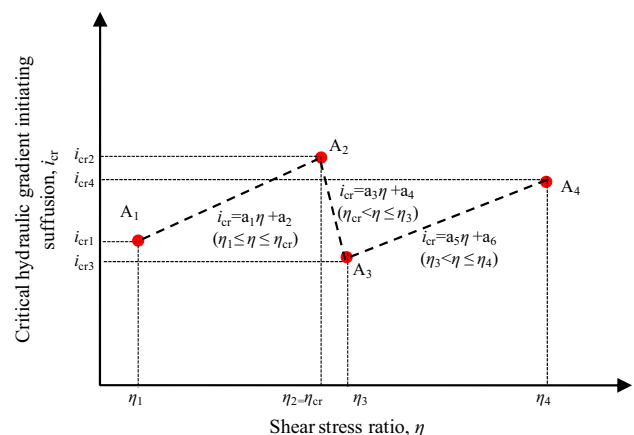

Fig. 7 Illustration of the empirical method determining the critical hydraulic gradients under complex stress states

The empirical method can be applied to the design of high earthen and rockfill dams constructed on internally unstable soils, and it can significantly reduce the numbers of suffusion tests, and only four suffusion tests and one consolidated drained triaxial compression test are needed to determine the critical hydraulic gradient under the same confining pressure.

4 Summary and conclusions

Thirty-six suffusion tests on three gap-graded and one broadly graded cohesionless soils, and four triaxial compression tests on the four original soils without suffusion were carried out to investigate the effect of deviator stress or shear stress ratio on the critical hydraulic gradient initiating suffusion. The main conclusions from this study can be summarized as follows:

The deviator stress or shear stress ratio has significant influence on the initiation of suffusion. The relationship between shear stress ratio and critical hydraulic gradient is piecewise linear. The critical hydraulic gradient first linearly increases with the increase in shear stress ratio, and it reaches the maximum value at the critical shear stress ratio, then it decreases suddenly and significantly, finally it increases linearly again with the increase in shear stress ratio. In this study, the relationship between shear stress ratio and critical hydraulic gradient was not completely consistent with that observed by Chang and Zhang [7].

There is a critical shear stress ratio for different internally unstable soils. The critical shear stress ratio is not the division between volumetric contraction and dilation, but it is the point where $\Delta V/\Delta q$ reaches the maximum value in the oscillation zone. For soils A, B, C, and D in this study, the critical shear stress ratios determined by suffusion tests are 1.11, 1.11, 1.20, and 1.0, respectively, whereas those determined by consolidated drained triaxial compression tests are 1.11, 1.13, 1.20, and 0.96, respectively, they are significantly consistent. Therefore, the critical shear stress ratio can be determined by a consolidated drained triaxial compression test.

Compared with the results in this study and Chang and Zhang [7], it was found that for different internally unstable soils with different grain size distributions and fine particle contents, the effect of deviator stress or shear stress ratio on the critical hydraulic gradient seemed to be similar. Based on this characteristic, an empirical method determining the critical hydraulic gradients under complex stress states was developed.

References

1. ASTM (2009) Standard test methods for particle-size distribution (gradation) of soils using sieve analysis. D6913-04, West Conshohocken
2. ASTM (2010) Standard test methods for measurement of hydraulic conductivity of saturated porous materials using a flexible wall permeameter. D5084-10, West Conshohocken
3. ASTM (2011) Standard test methods for the determination of the modulus and damping properties of soils using the cyclic triaxial apparatus. D3999/D3999 M-11, West Conshohocken
4. ASTM (2011) Standard test methods for consolidated drained triaxial compression test for soils. D7181-11, West Conshohocken
5. Benamar A, dos Santos RNC, Bennabi A, Karoui T (2019) Suffusion evaluation of coarse-graded soils from Rhine dikes. Acta Geotech 14:815–823. https://doi.org/10.1007/s11440-019-00782-1
6. Bendahmane F, Marot D, Alexis A (2008) Experimental parametric study of suffusion and backward erosion. J Geotech Geoenviron Eng 134:57–67. https://doi.org/10.1061/(ASCE)1090-0241(2008)134:1(57)
7. Chang DS, Zhang LM (2013) Critical hydraulic gradients of internal erosion under complex stress states. J Geotech Geoenviron Eng 139:1454–1467. https://doi.org/10.1061/(ASCE)GT.1943-5606.0000871
8. Chang DS, Zhang LM (2013) Extended internal stability criteria for soils under seepage. Soils Found 53:569–583. https://doi.org/10.1016/j.sandf.2013.06.008
9. Chang WJ, Chang CW, Zeng JK (2014) Liquefaction characteristics of gap-graded gravelly soils in K_0 condition. Soil Dyn Earthq Eng 56:74–85. https://doi.org/10.1016/j.soildyn.2013.10.005
10. El Dine BS, Dupla JC, Frank R, Canou J, Kazan Y (2010) Mechanical characterization of matrix coarse-grained soils with a large-sized triaxial device. Can Geotech J 47:425–438. https://doi.org/10.1139/t09-113
11. Evans MD, Zhou SP (1995) Liquefaction behavior of sand-gravel composites. J Geotech Eng ASCE 121:287–298. https://doi.org/10.1061/(ASCE)0733-9410(1995)121:3(287)
12. Flora A, Lirer S, Silvestri F (2012) Undrained cyclic resistance of undisturbed gravelly soils. Soil Dyn Earthq Eng 43:366–379. https://doi.org/10.1016/j.soildyn.2012.08.003
13. Hu Z, Zhang YD, Yang ZX (2019) Suffusion-induced deformation and microstructural change of granular soils: a coupled CFD-DEM study. Acta Geotech 14:795–814. https://doi.org/10.1007/s11440-019-00789-8
14. Ke L, Takahashi A (2012) Strength reduction of cohesionless soil due to internal erosion induced by one-dimensional upward seepage flow. Soils Found 52:698–711. https://doi.org/10.1016/j.sandf.2012.07.010
15. Ke L, Takahashi A (2014) Experimental investigations on suffusion characteristics and its mechanical consequences on saturated cohesionless soil. Soils Found 54:713–730. https://doi.org/10.1016/j.sandf.2014.06.024
16. Kenney TC, Lau D (1985) Internal stability of granular filters. Can Geotech J 22:215–225. https://doi.org/10.1139/t86-068
17. Ladd RS (1978) Preparing test specimens using undercompaction. Geotech Test J 1:16–23. https://doi.org/10.1520/GTJ10364J

18. Le VT, Marot D, Rochim A, Bendahmane F, Nguyen HH (2018) Suffusion susceptibility investigation by energy-based method and statistical analysis. Can Geotech J 55:57–68. https://doi.org/10.1139/cgj-2017-0024

19. Li M, Fannin RJ (2008) Comparison of two criteria for internal stability of granular soil. Can Geotech J 45:1303–1309. https://doi.org/10.1139/T08-046

20. Li M, Fannin RJ (2012) A theoretical envelope for internal instability of cohesionless soil. Géotechnique 62:77–80. https://doi.org/10.1680/geot.10.T.019

21. Liang Y, Yeh TCJ, Wang JJ, Liu MW, Zha YY, Hao YH (2017) Onset of suffusion in upward seepage under isotropic and anisotropic stress conditions. Eur J Environ Civ Eng. https://doi.org/10.1080/19648189.2017.1359110

22. Luo YL, Nie M, Xiao M (2017) Flume-scale experiments on suffusion at the bottom of cutoff wall in sandy gravel alluvium. Can Geotech J 54:1716–1727. https://doi.org/10.1139/cgj-2016-0248

23. Luo YL, Qiao L, Liu XX, Zhan ML, Sheng JC (2013) Hydromechanical experiments on suffusion under long-term large hydraulic heads. Nat Hazards 65:1361–1377. https://doi.org/10.1007/s11069-012-0415-y

24. Marachi ND, Chan CK, Seed HB (1972) Evaluation of properties of rockfill materials. J Soil Mech Div ASCE 98:95–114. https://doi.org/10.1016/S1002-0721(14)60184-8

25. Moffat RM, Fannin RJ (2011) A hydromechanical relation governing the internal stability of cohesionless soil. Can Geotech J 48:413–424. https://doi.org/10.1139/T10-070

26. Moffat RM, Fannin RJ, Garner SJ (2011) Spatial and temporal progression of internal erosion in cohesionless soil. Can Geotech J 48:399–412. https://doi.org/10.1139/T10-071

27. Moffat R, Herrera P (2015) Hydromechanical model for internal erosion and its relationship with the stress transmitted by the finer soil fraction. Acta Geotech 10:643–650. https://doi.org/10.1007/s11440-014-0326-z

28. Nguyen CD, Benahmed N, Andò E, Sibille L, Philippe P (2019) Experimental investigation of microstructural changes in soils eroded by suffusion using X-ray tomography. Acta Geotech 14:749–765. https://doi.org/10.1007/s11440-019-00787-w

29. Sibille L, Marot D, Sail Y (2015) A description of internal erosion by suffusion and induced settlements on cohesionless granular matter. Acta Geotech 10:735–748. https://doi.org/10.1007/s11440-015-0388-6

30. Skempton AW, Brogan JM (1994) Experiments on piping in sandy gravels. Géotechnique 44:449–460. https://doi.org/10.1680/geot.1994.44.3.449

31. To P, Scheuermann A, Williams DJ (2018) Quick assessment on susceptibility to suffusion of continuously graded soils by curvature of particle size distribution. Acta Geotech 13:1241–1248. https://doi.org/10.1007/s11440-017-0611-8

32. Wan CF, Fell R (2004) Experimental investigation of internal instability of soils in embankment dams and their foundations. UNICIV Rep. R429, the Univ. of New South Wales, Sydney

33. Wan CF, Fell R (2008) Assessing the potential of internal instability and suffusion in embankment dams and their foundations. J Geotech Geoenviron Eng 134:401–407. https://doi.org/10.1061/(ASCE)1090-0241(2008)134:3(401)

34. Yang J, Yin ZY, Laouafa F, Hicher P-Y (2019) Modeling coupled erosion and filtration of fine particles in granular media. Acta Geotech 5:5. https://doi.org/10.1007/s11440-019-00808-8

35. Zhang FS, Li ML, Peng M, Chen C, Zhang LM (2019) Three-dimensional DEM modeling of the stress-strain behavior for the gap-graded soils subjected to internal erosion. Acta Geotech 14:487–503. https://doi.org/10.1007/s11440-018-0655-4